National Défense
Defence nationale

IMAGE SMEARING IN A QUANTUM WELL INFRARED PHOTODETECTOR INTEGRATED WITH A LIGHT EMITTING DIODE

by

Shen Chiu and Emmanuel Dupont

19990126 017

DEFENCE RESEARCH ESTABLISHMENT OTTAWA
REPORT NO. 1339

DTIC QUALITY INSPECTED 3

Canada

DISTRIBUTION STATEMENT A
Approved for public release;
Distribution Unlimited

December 1998
Ottawa

AQ F99-04-0701

National Defence / Défense nationale

IMAGE SMEARING IN A QUANTUM WELL INFRARED PHOTODETECTOR INTEGRATED WITH A LIGHT EMITTING DIODE

by

Shen Chiu
Space Systems Group
Space Systems & Technology Section

and

Emmanuel Dupont
Advanced Devices Group
Institute for Microstructural Sciences
National Research Council

DEFENCE RESEARCH ESTABLISHMENT OTTAWA
REPORT NO. 1339

PROJECT
5EF12

December 1998
Ottawa

Abstract

The recent advances in infrared sensing technology has made it possible to use infrared sensors to support environmental observations, surveillance, threat detection, tracking, and target identification. For ballistic missile defence (BMD) related applications, the most important detector requirements are: high sensitivity, high uniformity, large format, and multicolor capabilities. Quantum well infrared photodetector (QWIP) is a relatively new candidate technology for BMD applications. It has become one of the most promising near-term infrared technologies to meet mid-course detection requirements because of its wavelength flexibility in mid-infrared, far-infrared, and very far-infrared regions, as well as multicolor capabilities. Canadian QWIP technology is based on monolithic integration of quantum well infrared photodetector with a light emitting diode (QWIP-LED), and was pioneered by Dr. H.C. Liu of Institute for Microstructural Sciences, National Research Council of Canada. The goal of the present program is to realize a 1×1 cm^2 two-color QWIP-LED imaging device by March 2001 and, eventually, to develop a very large format (up to 4×4 cm^2) prototype imaging camera.

The success of the QWIP-LED depends critically on the extent of spatial lateral spreading of both photocurrent generated in the QWIP and near infrared photons emitted by the LED as they escape from the QWIP-LED layers. According to a LED model proposed by Schnitzer *et al.*, there appears to be a trade-off between a high LED external quantum efficiency and a small photon lateral spread, the former being a necessary condition for achieving high detector sensitivity. The model predicts that as much as 25 reincarnations of the originally emitted NIR photons (as they spread laterally within the QWIP-LED) are required for most of the LED emitted light to escape. This lateral spreading due to multiple reflections and reincarnations of the NIR photons could potentially degrade the image quality or resolution of the QWIP-LED device. By adapting Schnitzer's model to the QWIP-LED structure, we have identified device parameters that could potentially influence the NIR photon lateral spread and the LED external efficiency. To achieve a high LED external efficiency we have found that the thickness of the LED active layer had to be significantly increased. Also, any additional absorption by anti-reflective coatings could have detrimental effects on the LED external efficiency. In addition, we have developed a simple sequential model to estimate the crosstalk between the incoming far (or mid) infrared image and the up-converted near infrared image. We found that the thickness of the LED is an important parameter that needs to be optimized in order to maximize the external efficiency and to minimize the crosstalk. A 6000 Å thick LED active layer should give a resolution of ~30 μm and an external efficiency of 10 to 15%.

DTIC QUALITY INSPECTED 3

Résumé

Les récents développements dans la technologie des senseurs à infrarouge ont rendu possible son utilisation dans les domaines de l'observation environnementale, de la surveillance, de la détection de menaces, de la poursuite, et de l'identification de cibles. Pour les applications reliées à la défense contre les missiles balistiques (BMD), les principales exigences pour le détecteur sont : une grande sensibilité, une grande uniformité, un format large, et des capacités multicolores. Le photodétecteur infrarouge à puits quantique (QWIP) est une technologie candidate relativement nouvelle pour les applications BMD. Cette technologie infrarouge est la plus prometteuse à court terme pour rencontrer les besoins de détection en mi-course à cause de sa flexibilité de longueur d'onde dans les régions de l'infrarouge moyen (MIR), de l'infrarouge lointain (FIR), et de l'infrarouge très lointain (VFIR), ainsi que de ses capacités multicolores. La technologie QWIP canadienne est basée sur l'intégration monolithique du photodétecteur infrarouge à puits quantique avec une diode électroluminescente (QWIP-LED). Cette technologie fut initiée par le Dr H.C. Liu, de l'Institut des sciences des microstructures du Conseil national de recherches du Canada. Le but du programme est présentement de réaliser un dispositif de formation d'images QWIP-LED deux couleurs de 1x1 cm^2, d'ici mars 2001, et éventuellement de développer un prototype de très grand format (jusqu'à 4x4 cm^2).

Le succès du QWIP-LED dépend essentiellement de l'étendue de la dispersion latérale spatiale du courant photoélectrique généré par le QWIP et des photons dans le proche infrarouge émis par le LED lorsqu'ils s'échappent des couches du QWIP-LED. Un modèle de LED proposé par Schnitzer *et al.* offre un compromis entre la grande efficacité quantique externe du LED et la faible dispersion latérale des photons, la première caractéristique étant nécessaire pour assurer au détecteur sa grande sensibilité. Le modèle prédit que jusqu'à 25 réincarnations des photons dans le proche infrarouge émis à l'origine (car ils se dispersent latéralement à l'intérieur du QWIP-LED) pour que la majeure partie de la lumière du LED puisse s'échapper. Cette dispersion latérale causée par les multiples réflexions et réincarnations des photons dans le proche infrarouge risque de nuire à la qualité et à la résolution d'image du dispositif QWIP-LED. En adaptant le modèle de Schnitzer à la structure du QWIP-LED, nous avons pu déterminer les paramètres du dispositif susceptibles d'influer sur la dispersion latérale des photons dans le proche infrarouge et l'efficacité externe du LED. Pour assurer la grande efficacité externe du LED, nous avons découvert que l'épaisseur de la couche active du LED devait être beaucoup augmentée. De plus, toute absorption supplémentaire par les couches antiréfléchissantes (AR) risque de nuire à l'efficacité externe du LED. Nous avons, en outre, conçu un modèle séquentiel simple afin d'évaluer la diaphonie entre l'image dans l'infrarouge lointain (ou intermédiaire) qui est reçue et l'image dans le proche infrarouge convertie à la fréquence supérieure. Nous avons trouvé que l'épaisseur du LED est un paramètre important qu'il faut optimiser pour maximiser l'efficacité externe et minimiser la diaphonie. Un LED doté d'une épaisse couche active de 6000 Å devrait offrir une résolution de ~30 μm et une efficacité de 10 à 15 %.

Executive Summary

The success of the Quantum Well Infrared Photodetector integrated with a Light Emitting Diode (QWIP-LED) depends on the extent of spatial lateral spreading of both photocurrent generated in the QWIP and near infrared photons emitted by the LED as they escape from the QWIP-LED layers. In order to model the behavior of the NIR photons in the QWIP-LED layers, we have adapted Schnitzer's LED model for our QWIP-LED structure and have derived an expression for the QWIP-LED external efficiency. We calculated the external efficiency $\eta_{ext,fiberbundle}$ and the image resolution as a function of the absorption $\alpha_o d_o$ in the LED active layer and the parasitic absorption $\alpha_i d_i$ in the contact layers, for a QWIP-LED bonded to a fiber optics faceplate. Several scenarios have been considered:

For an ideal transmissive QWIP-LED — with a 100% internal efficiency, a 6000 Å thick active layer, a 1% contact absorption, and perfect coatings — we could achieve an external efficiency of about 17%. The crosstalk would be about 30 μm, which is the maximum we can afford (since the pseudo pixel size will be about 30 μm). The thickness of the LED active layer was shown to play a major role in reducing the crosstalk. However, the diffusion length of the carriers in the LED (μm range) limits the maximum LED thickeness to ~6000 Å.

When the LED active layer is thin (200-1000 Å), the average absorption coefficient of the LED $\alpha_0' = \alpha_0 d_0 / e$ is smaller than $(1/p_e)\alpha_i d_i$. As a result the external efficiency is strongly reduced. Moreover, the mean distance between re-incarnations events (which scales with $1/\alpha_0'$) is very large and the crosstalk can be as bad as few hundreds of microns.

The effect of absorbing coatings was shown to be detrimental to achieving a high external efficiency. It does however reduce the crosstalk, but only at the expense of the external efficiency.

Our calculations have shown that if the coatings were not absorbing, even a 70% transmissive top coating and a 70% reflective bottom coating would have negligible effects on the external efficiency compared to the perfect coating case. We got a slightly reduced effective escape probability but the overall effect was almost negligible.

Finally, using a more pessimistic value of 95% for the internal efficiency and 80% R and T' coatings and assuming again non-absorbing top and bottom coatings, we found that the external efficiency was significantly reduced down to ~10 % level. This shows how sensitive the overall device performance is to the internal efficiency of the LED. With additional losses in the coatings, the external yield quickly drops to only a few %.

These results clearly indicate we will have to seriously consider bonding the QWIP-LED directly onto a CCD chip. Since the index of refraction of the CCD is very close to that of the LED, the escape cone will be significantly wider (~140°), allowing as much as 75-80% of the NIR light to escape at each emission event. This will not only drastically improve the external efficiency (up to 70-80%) but also will considerably reduce the crosstalk.

Table of Contents

List of Figures

1. Introduction

Infrared sensors find applications in all phases of ballistic missile defence (BMD). These include surveillance, threat detection, tracking, identification, discrimination, targeting and interception[1]. Airborne surveillance sensors used for tactical applications typically observe warm targets with high background irradiance from the heated windows, scattered sunlight, and the earth's surface. Such applications require accurate measurement and substraction of background irradiance to detect the target's signal. Space-based surveillance sensors — if used in a LIMB-looking configuration — typically see cool targets with low background irradiance levels. When the scene is a space background and the targets are at relatively low temperatures, far infrared (FIR, 8 to 12 μm) and very far infrared (VFIR, >12 μm) are wavelengths of choice. For airborne applications, the most important wavebands are determined by the atmospheric transmission windows; these are mid infrared (MIR, 3 to 5 μm) and far infrared (8-12 μm). Thus, a BMD requirement for infrared detectors is wavelength flexibility from MIR to VFIR. In addition, the following have been identified as equally important BMD requirements for a infrared sensor: high sensitivity, high uniformity, large format, and multicolour capabilities.

Quantum well infrared photodetector (QWIP) is a relatively new candidate technology for ballistic missile defence applications. It has become one of the most promising near-term infrared technologies to meet the BMD requirements[1] because of its wavelength flexibility in MIR, FIR, and VFIR regions, as well as multicolour capabilities.

Canadian QWIP technology is based on monolithic integration of quantum well infrared photodetector with a light emitting diode (QWIP-LED), and was pioneered by Dr. H.C. Liu[2] of Institute for Microstructural Sciences, National Research Council of Canada. The program is supported mainly by two Canadian Defence Research Establishments, Valcartier and Ottawa, and its goal is to realize a 1×1 cm^2 two-color QWIP-LED imaging device by March 2001 and, eventually, to develop a very large format (up to 4×4 cm^2) prototype imaging camera.

The operation of the QWIP-LED device is based on direct injection of carriers photoexcited in the QWIP by mid or far infrared (M/FIR) radiation into the LED active region and subsequent emission of near infrared (NIR) radiation (see Fig. 1). Thus, the QWIP-LED operates as a converter of M/FIR to NIR light.

An important technological advantage of the QWIP-LED approach is that it allows fabrication of large two-dimensional focal plane arrays (FPAs) with NIR output which can be easily imaged by well developed devices such as Si CCDs. This approach eliminates the need for hybrid integration of QWIP with a Si readout circuit — an approach taken by all other QWIP research groups — and its associated thermal mismatch problems (particularly for a very large FPA format).

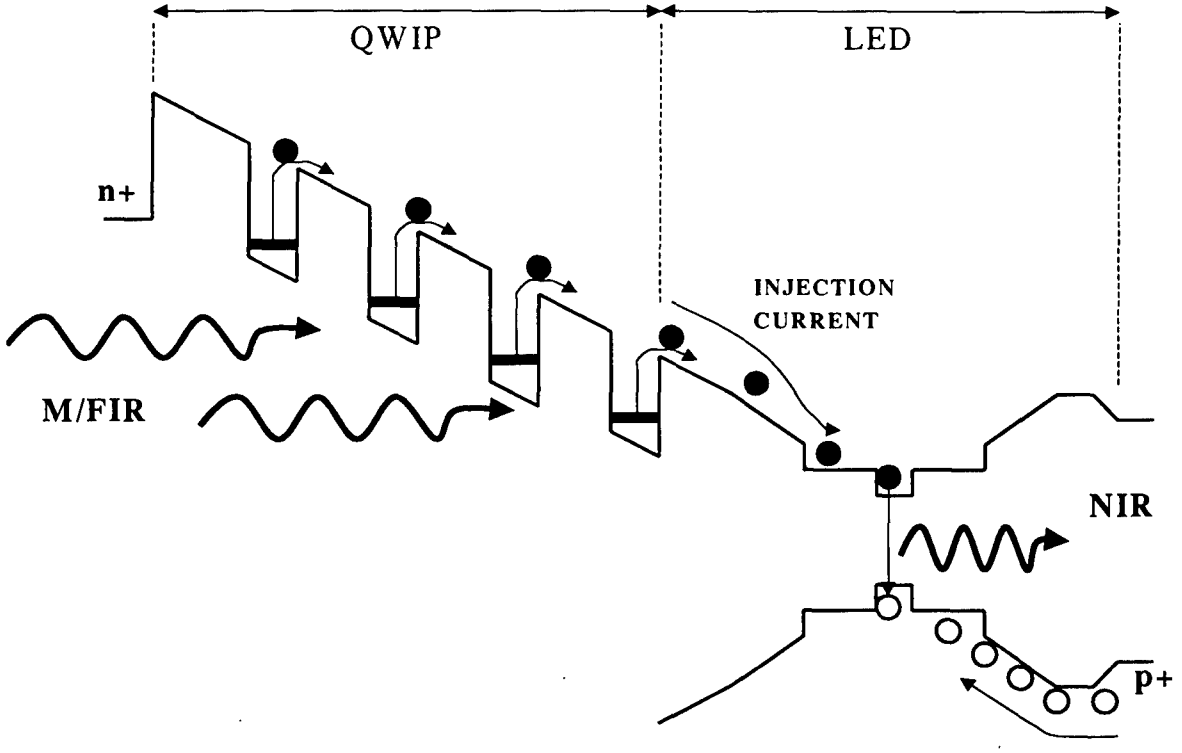

Fig. 1 Schematic diagram of band profile and physical processes in a QWIP-LED.

A necessary condition for successful operation of the QWIP-LED device is a small spatial smearing of the incoming M/FIR image in its transformation into the LED NIR emission image. The spatial resolution of the device is determined by a number of factors. These include lateral spreading of photocurrent in the QWIP (i.e., in-plane diffusion of carriers injected into the LED) and lateral spreading of NIR photons emitted by the LED as they escape from the QWIP-LED layers. The former was investigated by Ershov *et al.*[3,4] and was shown to introduce negligible image distortion.

The goal of the present work is to investigate the latter factor, i.e., to determine major device parameters influencing the NIR light lateral spread and the LED external efficiency, and their impact on the image quality of the QWIP-LED device.

2. External Efficiency of the LED

In order to achieve high detector sensitivity, it is important to optimize the QWIP-LED output, which depends on the external quantum efficiency (QE) of the integrated LED. The internal QE of III-V double heterostructure LED can be well over 90%[5]. However, this high internal yield must be converted into useful external output. In general, the external QE of LEDs is rather poor, typically only a few percent. The reason for this low output is that the semiconductor refractive index is rather high (n ~ 3.54 in GaAs), leading to a very narrow escape cone for the isotropic spontaneous emission of NIR light from GaAs into air.

The 16° half cone angle imposed by Snell's Law covers a solid angle of only ~ $(1/4n^2)\times 4\pi$ steradians. For GaAs this translates into an external efficiency of ~2%.

In order to maximize the LED external yield, Schnitzer *et al.*[6] has proposed and realized an optically thin AlGaAs/GaAs/AlGaAs double heterostructure LED mounted on a high reflectivity surface which showed impressive internal and external QEs of 99.7% and 72%, respectively. The 72% external efficiency was based on an optically pumped LED, which eliminated the need for two additional heavily doped n^+ and p^+ contact layers. For an electrically pumped LED, the additional contact layers introduced free-carrier absorption loss which resulted in a reduced external QE of ~50%.

According to Schnitzer's model once a NIR photon is emitted in the LED active layer, it can have one of several possible destinies: (a) It can escape through the escape cone at the top of the double heterostructure; (b) it can be reabsorbed by the parasitic optical losses in the structure (e.g., at the bottom reflector); (c) it can be reabsorbed in the LED active layer and experience reincarnation as a photon. If the internal QE were high and if there were no parasitic optical losses, the photon would be reincarnated many times, having a 2% probability (for GaAs/Air interface) of finding the escape cone each time.

The key to Schnitzer's success lies in the recycling of reflected photons (i.e., photons that are outside escape cone), and small nonradiative and parasitic optical losses. According to the model[5] as much as 25 reincarnation events are required for most of the LED emitted photons to escape. However, with multiple reflections and reincarnations of the NIR photons, one runs into a different problem — that of the lateral spreading of photons and the potential image distortion.

3. External Efficiency of QWIP-LED

In order to model the behavior of the NIR photons in the QWIP-LED layers, we have adapted Schnitzer's model for our QWIP-LED structure (see Fig. 2). Our QWIP-LED device is firstly bonded to a carrier substrate and subsequently thinned down from the back to completely remove the original GaAs substrate by a combination of mechanical polishing and wet etching techniques. The details of the substrate removal process will be published elsewhere[7]. The removal of the substrate is necessary to maximize the QWIP-LED output and to operate the device in the so-called "transmissive mode" (i.e., the incoming M/FIR light is incident on one side of the device and the resulting NIR image is output at the other side as opposed to the "reflective mode," where both input and output take place on a same side).

For our QWIP-LED structure, the top and bottom surfaces are coated with anti-reflective (AR) coatings. The adapted model takes into account additional effects due to the imperfect AR coatings and the optical glue needed for bonding the QWIP-LED onto the carrier substrate. For our first prototype transmissive QWIP-LED camera, the NIR output will be imaged by a CCD chip via a fiber optics faceplate. Thus, for the purpose of this analysis we assume the carrier substrate to be a fiber faceplate with a numerical aperture NA = 1.

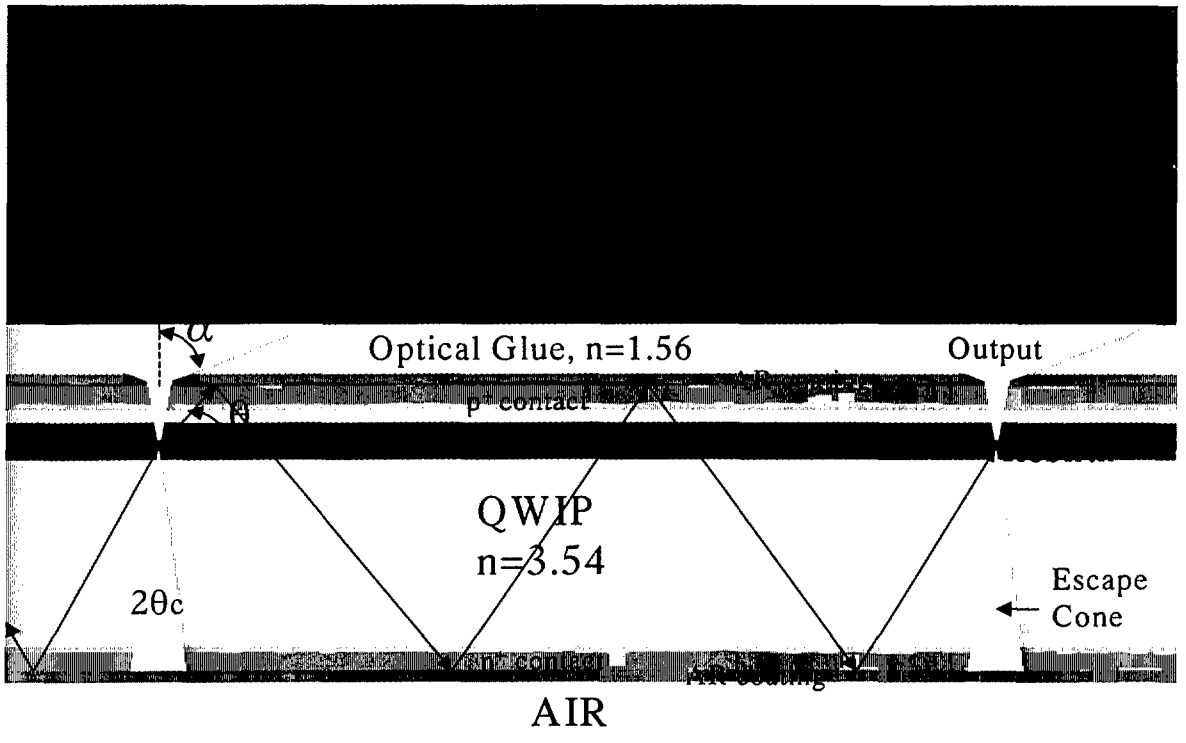

Fig. 2 Schematic of QWIP-LED layer structure showing NIR emission and absorption/reemission (rebirth) events.

Because of absorption the top coating (probably Fabry-Perot type or ITO film) will not allow 100% transmission even at angles less than the critical angle θ_c (= Arcsin(1.56/3.54) ≈ 25°). Similarly for the multilayer bottom coating, the reflection will be less than 100% within the $2\theta_c$ escape cone. Also, it is important to note that even though the light with an incidence angle < 25° can escape from the sample, we will only be able to detect the rays below ~17° because of the numerical aperture (NA = $n_{opticglue}\sin\alpha$ = 1; see Fig. 2) of the fiber optics faceplate. Our calculations take this effect into account and also includes the transmission efficiency of the faceplate (typically 60%). Because of the finite NA of the fibers we loose about a factor of 2 (= $n_{opticglue}^2$) in the external efficiency, and almost a factor of 4 if we include the transmission coefficient. This is why we should investigate the solution for bonding the QWIP-LED directly onto the CCD chip.

4. QWIP-LED Model

Assuming isotropic emission, the 25° half angle cone represents only ~9% [= $1/(2(n_{gaas}/n_{opticglue})^2)$] of the spontaneous radiation. We call this value p_e for escape probability. Because of finite reflectivity of the top coating, the light emitted in this cone can bounce back and forth between the two surfaces and will experience some additional loss. Therefore, the actual escape probability p_e' within the 25° half cone is smaller than p_e. In a single pass the attenuation of the trapped light (in the cone) is:

$$a = \exp(-\alpha_i d_i - ((1-\eta_{int}) + \eta_{int}(1-p_e))\,\alpha_o d_o), \quad (1)$$

where $\alpha_i d_i$ is the parasitic absorption in all layers (mainly the contacts) except the LED, $\alpha_0 d_0$ is the absorption of the LED active layer (~5000 cm^{-1}), and η_{int} is the internal QE of the LED. In this expression $\eta_{int}(1-p_e)\alpha_0 d_0$ represents the light which is absorbed again in the LED during the multi-bounce process and re-emitted outside the cone. The second term $(1-\eta_{int})\alpha_0 d_0$ represents a small portion of the light which is lost in the LED via nonradiative processes.

The average escape probability p_e' of the light inside the 2×25° cone is simply given by a multi-bounce calculation:

$$\begin{aligned} p_e' &= \frac{p_e}{2}\left\{T' + T'(1-T'-A')Ra^2 + T'\left((1-T'-A')Ra^2\right)^2 + \ldots\right\} \\ &+ \frac{p_e}{2}\left\{Ra^2T' + Ra^2T'(1-T'-A')Ra^2 + Ra^2T'\left((1-T'-A')Ra^2\right)^2 + \ldots\right\} \\ &= \frac{p_e}{2}(1+Ra^2)\frac{T'}{1-(1-T'-A')Ra^2}, \end{aligned} \quad (2)$$

where T' is the transmission coefficient of the top coating at small angles (< 25°), A' is the absorption of the top coating, and R is the reflection coefficient of the bottom coating at small angles (above 16° there is a total internal reflection at the GaAs/Air interface). For reasonable values of R(0.9 to 1.0), T'(0.9 to 1.0), A'(<0.1), and small values of a ($\alpha_0 d_0$ up to 0.2) p_e' is close to p_e.

Using the same analysis as Schnitzer, we calculate the external efficiency of the substrate thinned transmissive QWIP-LED:

$$\eta_{ext} = \frac{p_e'\eta_{int}\alpha_0 d_0}{p_e'\eta_{int}\alpha_0 d_0 + (1-\eta_{int})\alpha_0 d_0 + \alpha_i d_i + \frac{(A+A')}{4}(1-\sin^2\theta_c)}, \quad (3)$$

where A is the absorption of the bottom coating above the critical angle. When taking into account the fiber bundle faceplate, we multiply this expression by:

$$\eta_{ext,\,fiberbundle} = \frac{T_{fiberbunll\ e}}{n^2_{opticglue}}\eta_{ext}, \quad (4)$$

where $T_{fiberbundle}$ is the transmissive coefficient of the faceplate and $n_{opticglue}$ is the refractive index of the glue.

5. 1-D Sequential Model for an Estimation of the Crosstalk

Our method is first to estimate a mean distance d between two absorption-reemission events. Before carrying out this calculation we know that this distance should be close to the inverse of the average LED absorption coefficient. For simplicity we assume that the NIR photons of the initial pool (generation "0") created by the M/FIR light will travel only in two directions: right and left (i.e., assuming a 1-D model). We then follow the number of photons as they travel along the microcavity (see Fig. 2), experience re-incarnations in the

LED active layer, get absorbed in the contacts or imperfect mirrors, get lost in nonradiative processes ($\eta_{int}<1$)...etc. [We note that we are using a 1-D model as an approximation to the 2-D problem, where in reality NIR photons spread laterally in two dimensions within the microcavity.]

Fig. 3 represents the evolution of the number of photons inside the cavity versus the propagation distance. We want to calculate the mean propagation distance *d* that a photon outside the escape cone will travel before it gets absorbed in the LED and re-emitted. To do so we have to find an equivalent mean exponential decay of the number of photons over several reincarnation events (see Fig. 3).

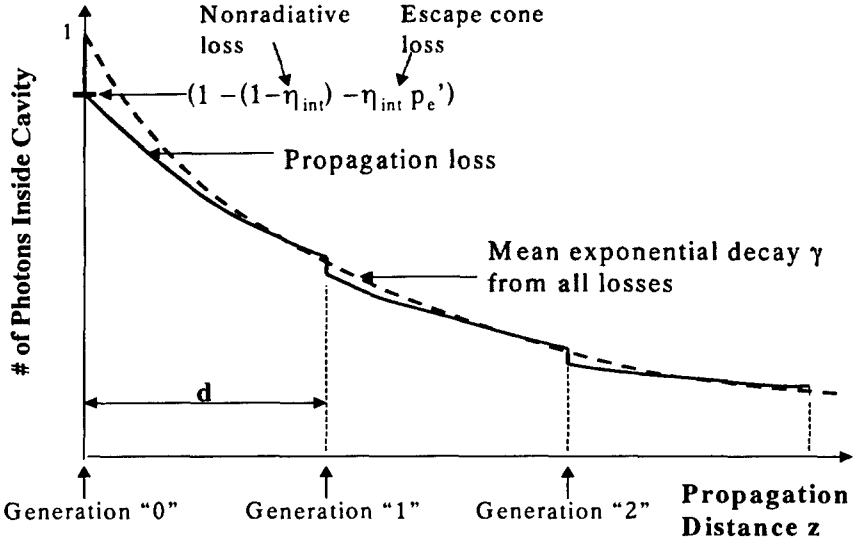

Fig. 3 Population of photons as they travel along the microcavity from the original location of emission (Generation "0").

When N photons travel a distance *dx* , $N\alpha_0'dx$ are absorbed by the LED, where α_0' is an mean absorption coefficient, $\alpha_0'=\alpha_0(d_0/e)$, averaged over the total thickness e of the QWIP-LED device. [Here we define a new absoption coefficient because in our QWIP-LED structure, the LED layer is only a fraction of the total QWIP-LED thickness.] From these absorbed photons, $N\alpha_0'dx$, $(1-\eta_{int})N\alpha_0'dx$ are lost in nonradiative processes, $\eta_{int}N\alpha_0'dx$ are re-emitted as reincarnated photons, and $p_e'\eta_{int}N\alpha_0'dx$ escape via the 25° half angle cone. Thus, we again define a new absorption coefficient $\alpha_o'_{,distr}$ for losses due to the nonradiative processes and the photon escape via the $2\theta_c$ cone:

$$\alpha_o'_{,distr} = ((1-\eta_{int}) + p_e'\eta_{int})\alpha_0'. \qquad (5)$$

At each bounce on a surface the light experiences some loss due to the imperfect AR coatings. Tus, the reflection coefficient above the critical angle at the top coating is R'=1-A' and at the bottom coating is R=1-A. Similarly, we can define an equivalent absorption coefficient for these reflection losses:

$$RR' = e^{-\alpha_{RR'} \cdot x} \Rightarrow \alpha_{RR'} = -\frac{\log(R \times R')}{x}, \tag{6}$$

where θ [$=(90^\circ-\theta_c)/2$] is the average angle of the rays outside the escape cone (see Fig. 2) and x is defined to be the actual distance traveled by a photon as it departs from one location in the LED active layer (birth place) to another location (in lateral direction) in the same layer. This involves two reflections, one at the top coating and the other at the bottom coating, and one single pass through the LED active layer. From a simple geometry x can be shown to be equal to:

$$x = \frac{2e}{\sin\theta}. \tag{7}$$

Thus, the equivalent absorption coefficient due to the top and bottom coatings is:

$$\alpha_{RR'} = -\frac{\log[(1-A)(1-A')]}{2e/\sin\theta}. \tag{8}$$

Finally putting together all the absorption terms, we obtain the overall absorption coefficient γ for the trapped photons:

$$\gamma = \left\{\left(1-\eta_{\text{int}}\right)+\eta_{\text{int}}\, p_e'\right\}\alpha_0\frac{d_0}{e}+\alpha_i\frac{d_i}{e}+\frac{\log(1-A')(1-A)}{2e/\sin\theta}. \tag{9}$$

Here γ is the exponential constant of the decaying dashed line shown in Fig. 3. We can therefore derive another expression for the QWIP-LED external efficiency by summing all the photons emitted via the escape cone at each multiple distance of d, where d is the mean distance between re-incarnations:

$$\eta_{ext} = p_e'\left\{1+e^{-\gamma d}+e^{-2\gamma d}+....\right\} = p_e'\frac{1}{1-e^{-\gamma d}}. \tag{10}$$

From this we derive d:

$$d = -\frac{\log\left(1-\frac{p_e'}{\eta_{ext}}\right)}{\gamma}. \tag{11}$$

We note that the η_{ext} expression is a discrete approximation to a continuous emission profile of NIR light. Its result may not be as accurate as that of the expression derived in Sec. 4. However, it does serve the purpose of estimating the lateral spread of photons as they experiece a chain of reincarnation events.

With non-absorbing coatings (A,A'=0) and for large external efficiencies the distance d is indeed about $(e/d_0)/\alpha_0$ as we expected. Then , it is straight forward to estimate the crosstalk. At each absorption-emission we say that 50% of photons goes to the left and 50% to the right. And from one emission event to the next absorption event we lose $1-\exp(-\gamma d)$ of trapped photons (see Fig. 3). Therefore from an initial pool of NIR photons

at z=0 (where z is the lateral propagation distance), generated by the M/FIR light via wavelength up-conversion, we can draw a photon propagation tree by following the population of trapped photons at each reincarnation event (see Fig. 4).

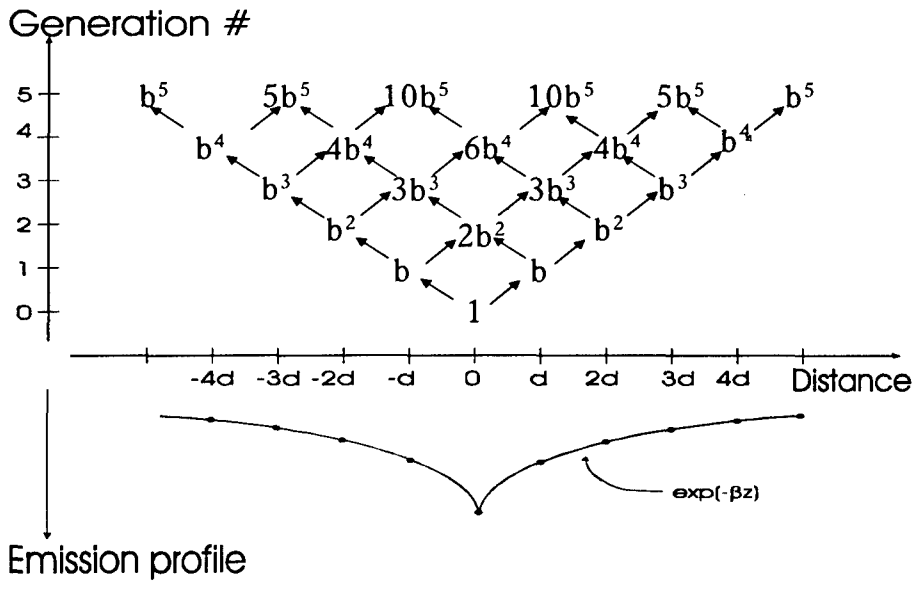

Fig. 4 Photon propagation tree showing different generations of photon reincarnations as a function of lateral propagation distance z.

The propagation tree shows how photons are distributed over the distance away from the "0-generation" position. The propagation distance z is expressed in units of *d*, the mean distance between reincarnations. The coefficient *b* represents the portion of the trapped photons that are left from the previous absorption/reemission event before another reincarnation event takes place; and it is equal to:

$$b = \frac{1}{2}e^{-\gamma d} = \frac{1}{2}\left(1 - \frac{p_e'}{\eta_{ext}}\right). \tag{12}$$

Thus, at z=0 the emission is equal to:

$$I(z=0) = p_e'\{1 + 2b^2 + 6b^4 + 20b^6 + 70b^8 + ...\}. \tag{13}$$

At z=d the emission is equal to:

$$I(z=d) = p_e'b\{1 + 3b^2 + 10b^4 + 35b^6 + ...\}. \tag{14}$$

At z=2d the emission is equal to:

$$I(z=2d) = p_e'b^2\{1 + 4b^2 + 15b^4 + 56b^6 + ...\}. \tag{15}$$

Assuming that the terms between the brackets {} do not change too quickly with z, we clearly see that the emission profile has an exponential behaviour.

Small external efficiencies:

When b is small (<<0.5), i.e. when the external effciency is not very large, the brackets {} are close to unity, and therefore the exponential is decreasing by a factor of b for every d distance. In this case the resolution will be better than $2d$. The exponential constant, β, of the decaying emission profile (see Fig. 4) is such that:

$$-\beta d = \log\left(0.5\exp\left(-\gamma d\right)\right) = -\log 2 + \log\left(1 - \frac{p_e'}{\eta_{ext}}\right). \tag{16}$$

And since the crosstalk is:

$$\text{Resolution} = \frac{2\cos(\theta)\log(2)}{\beta}, \tag{17}$$

we deduce that:

$$\text{Resolution} = 2\cos\theta\log 2\frac{1}{\gamma}\frac{-\log\left(1 - \frac{p_e'}{\eta_{ext}}\right)}{\log 2 - \log\left(1 - \frac{p_e'}{\eta_{ext}}\right)}. \tag{18}$$

Large external efficiencies:

On the other hand if the external efficiency is very high, b converges to 0.5 and the terms in the brackets become important. The exponential constant β converges to $1/(4.842\times d)$ and the resolution becomes:

$$\text{Resolution} = 2\times 4.84\times\cos\theta\times\log 2\times d\,. \tag{19}$$

With the optical glue, $\theta = 32^\circ$ and the crosstalk is :

$$\text{Resolution} = 5.67\times\frac{e}{\alpha_o d_o}. \tag{20}$$

General case:

In our simulations we calculated the emission profile up to z=5d and fit it with an exponential decay β. The ratio $1/\beta d$ is plotted against the ratio η_{ext}/p_e' (see Fig. 5). Since the coeffcient $2\times\log 2\times\cos\theta$ is close to 1, this plot gives us the approximate crosstalk. We know that the distance d is roughly the inverse of the averaged LED absorption coeffcient

$d=e/(\alpha_0 d_0)$. We see that the small external efficiency approximation is valid up to $\eta_{ext}=2\times p_e'$ only.

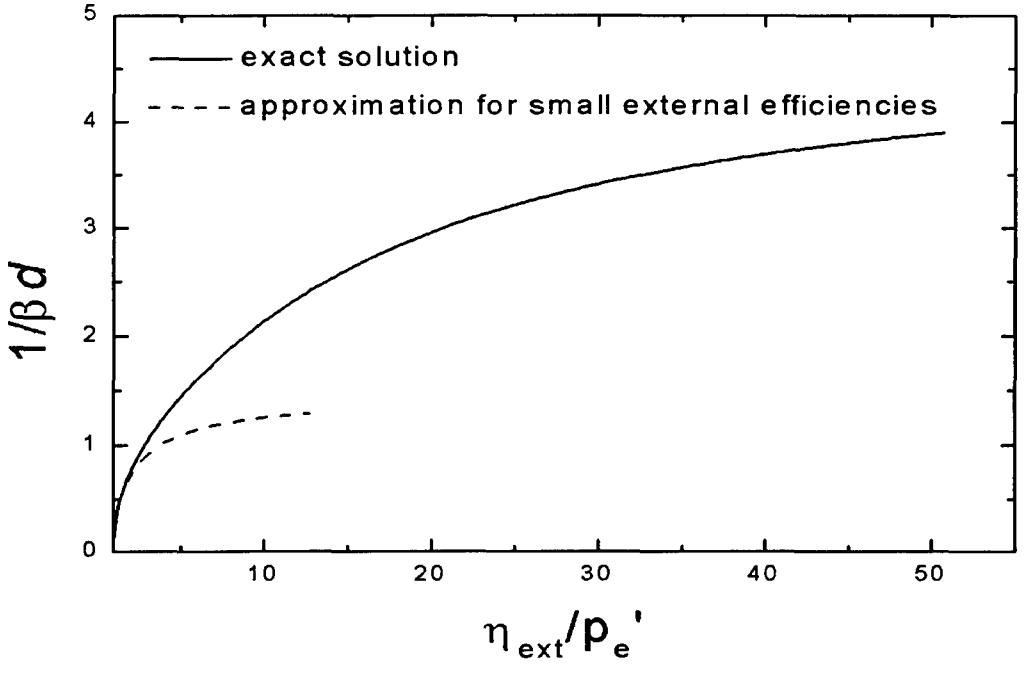

Fig. 5 The $1/\beta d$ is plotted against η_{ext}/p_e' showing that small η_{ext} approximation is valid up to $\eta_{ext}=2p_e'$.

6. Numerical Applications

We calculated the external efficiency $\eta_{ext,fiberbundle}$ of the QWIP-LED bonded to the fiber bundle faceplate, the mean distance d between re-incarnations events, the effective escape probability p_e', and the image resolution of the QWIP-LED as a function of the absorption $\alpha_0 d_0$ in the LED active layer and the parasitic absorption $\alpha_i d_i$ in the contact layers. The results are plotted in Figs. 6 to 10 for various scenarios. Using a LED absorption coefficient $\alpha_0 = 5\times10^3$ cm^{-1} as suggested by Schnitzer[5], then $\alpha_0 d_0 = 0.1$ would mean that the active layer is 2000 Å thick. The total QWIP-LED thickness e is ~3.3 μm as it was designed for our first transmissive QWP-LED device.

Ideal transmissive QWIP-LED:

Suppose that the internal efficiency η_{int} is 100% and that both the coatings are perfect, then we could achieve an external efficiency of about 17% with a 6000 Å thick active layer and a 1% contact absorption (see Fig. 6). The crosstalk would be about 30 μm, which is the maximum we can afford (since the pseudo pixel size will be about 30 μm). We clearly see that the thickness of the LED active layer is playing a major role in reducing the crosstalk;

however, the diffusion length of the carriers in the LED (μm range) is an upperbound we should avoid. This is why we did not use a thickness above 6000 Å.

Thin LED active layer means poor η_{ext} and a huge crosstalk:

In the case of a thin LED active layer (200 to 1000 Å), the average absorption coefficient of the LED $\alpha_0'=\alpha_0 d_0/e$ is smaller than $(1/p_e)\alpha_i d_i$; as a result the external efficiency is strongly reduced (see Fig. 7). Moreover, the mean distance between re-incarnations events (which scales with $1/\alpha_0'$) is very large and the crosstalk can be as bad as few hundreds of microns.

Influence of absorbing coatings — do not use Fabry-Perot filters!

The top AR coating as first designed by our Thin Films Group was a Ag/Si/Ag/Si Fabry-Perot filter. This type of coating could achieve a good transmission at near-infrared wavelengths and a high reflectance in the mid-infrared. However, the 80% transmission did not mean that 20% was reflected back and re-used in the microcavity. As a manner of fact, above the critical angle θ_c (~25°) the transmission was null but the reflectance was only 80% percent. The remaining 20% was lost in the Ag mirrors. This additionnal loss is detrimental to achieving a high external efficiency (see Fig. 8). It does, however, reduce the crosstalk, but only at the expense of the external efficiency. We are presently investigating other types of coatings such as Indium-Tin-Oxide (ITO) films. These are electrically conducting transparent coatings often used in flat panel display applications. They are transparent in the near-infrared but have a metallic behaviour in the mid infrared.

Tolerance on non-absorbing coatings:

Next, we carried out our calculations assuming a 70% transmissive top coating and a 70% reflective bottom coating (see Fig. 9). If the coatings were not absorbing, the effect was shown to be quite negligible compared to the perfect coating case (see Fig. 6). We got a slightly reduced effective escape probability but the overall effect was almost negligible.

More realistic η_{int} values and coatings:

Using a more pessimistic value of 95% for the internal efficiency and 80% R and T' coatings and assuming again non-absorbing top and bottom coatings, we found that the external efficiency was significantly reduced down to ~10 % level (see Fig.10). This shows how sensitive the overall device performance is to the internal efficiency of the LED. With additional losses in the coatings, the external yield quickly drops to only a few %.

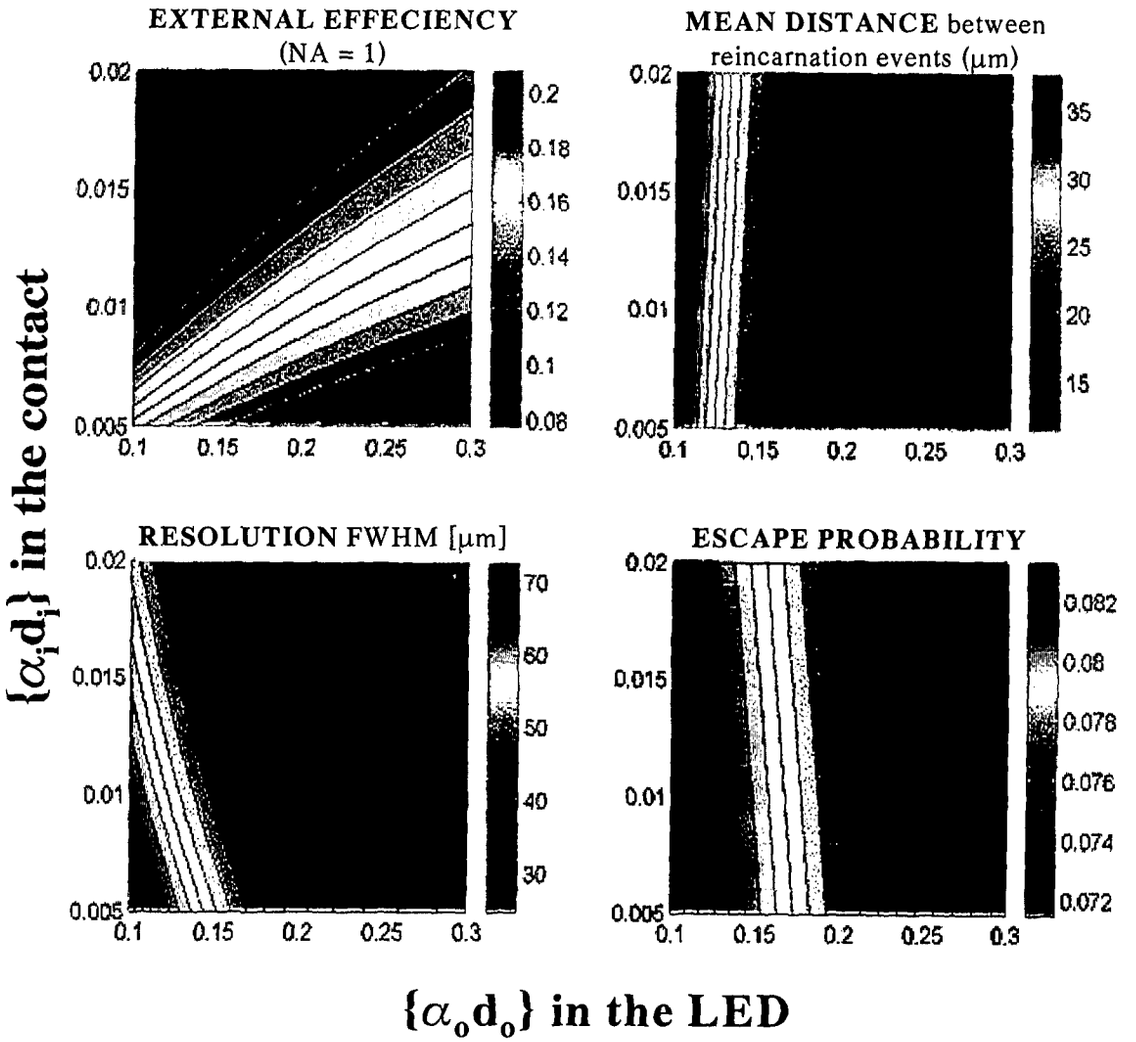

Fig. 6 Perfect coatings: $\eta_{int} = 0.999$, thick LED (2000 to 6000 Å), T' = 1 (0° to θ_c), A' = 0 (0° to 90°), R = 1 (0° to 17°), A = 0 (0° to 90°).

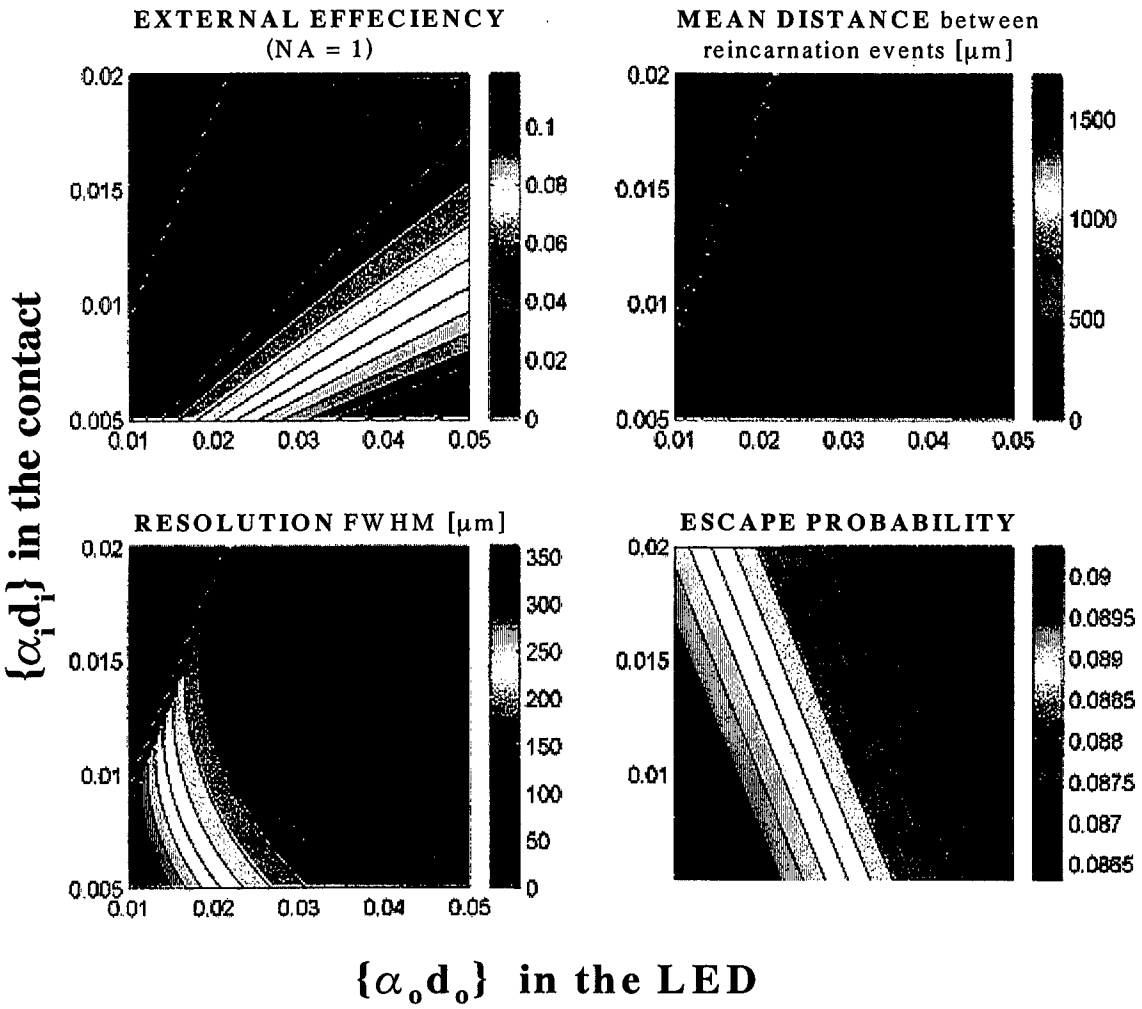

Fig. 7 Thin LED (200 to 1000 Å), $\eta_{int} = 0.999$, T' = 1 (0° to θ_c), A' = 0 (0° to 90°), R = 1 (0° to 17°), and A = 0 (0° to 90°).

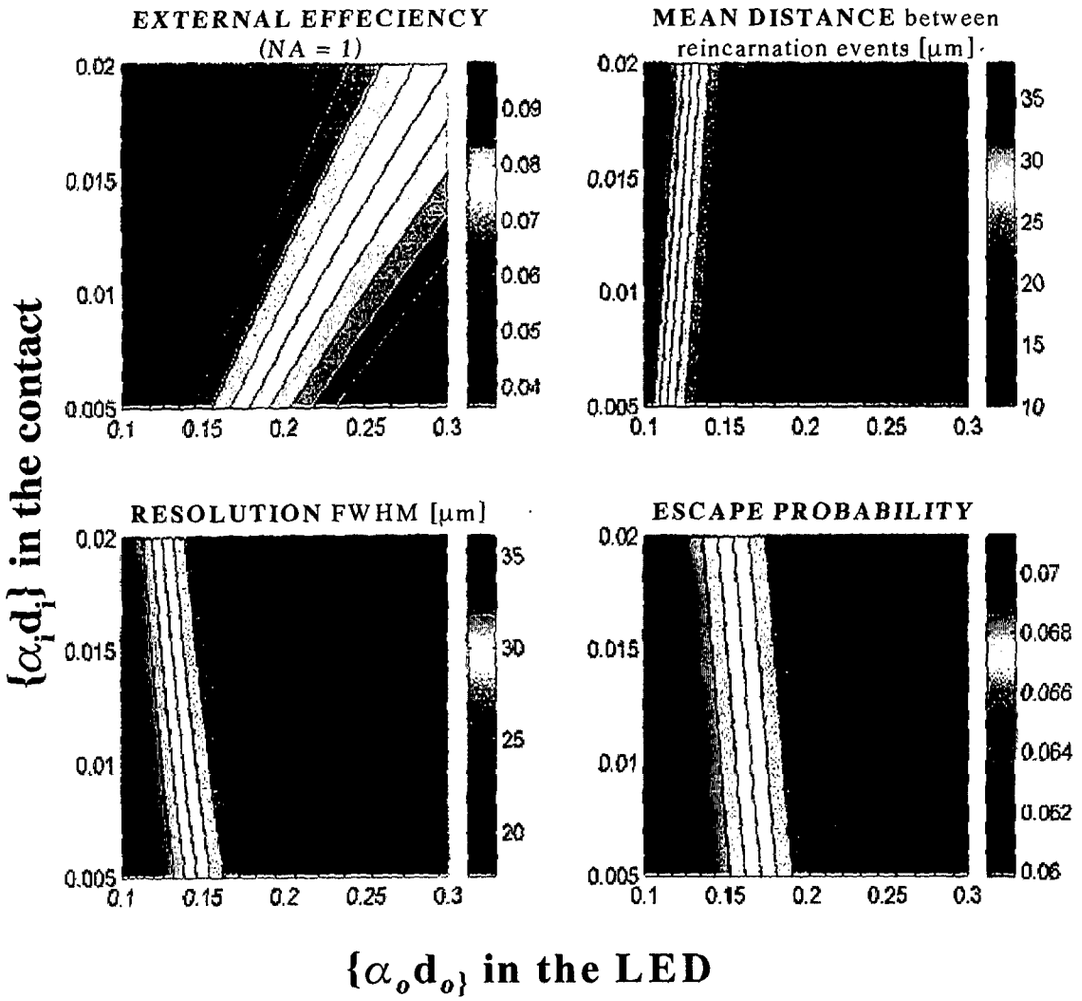

Fig. 8 Bad top coating: η_{int} = 0.999, T' = 0.8 (0° to θ_c), A' = 0.12 (0° to 90°), R = 1 (0° to 17°), and A = 0 (0° to 90°).

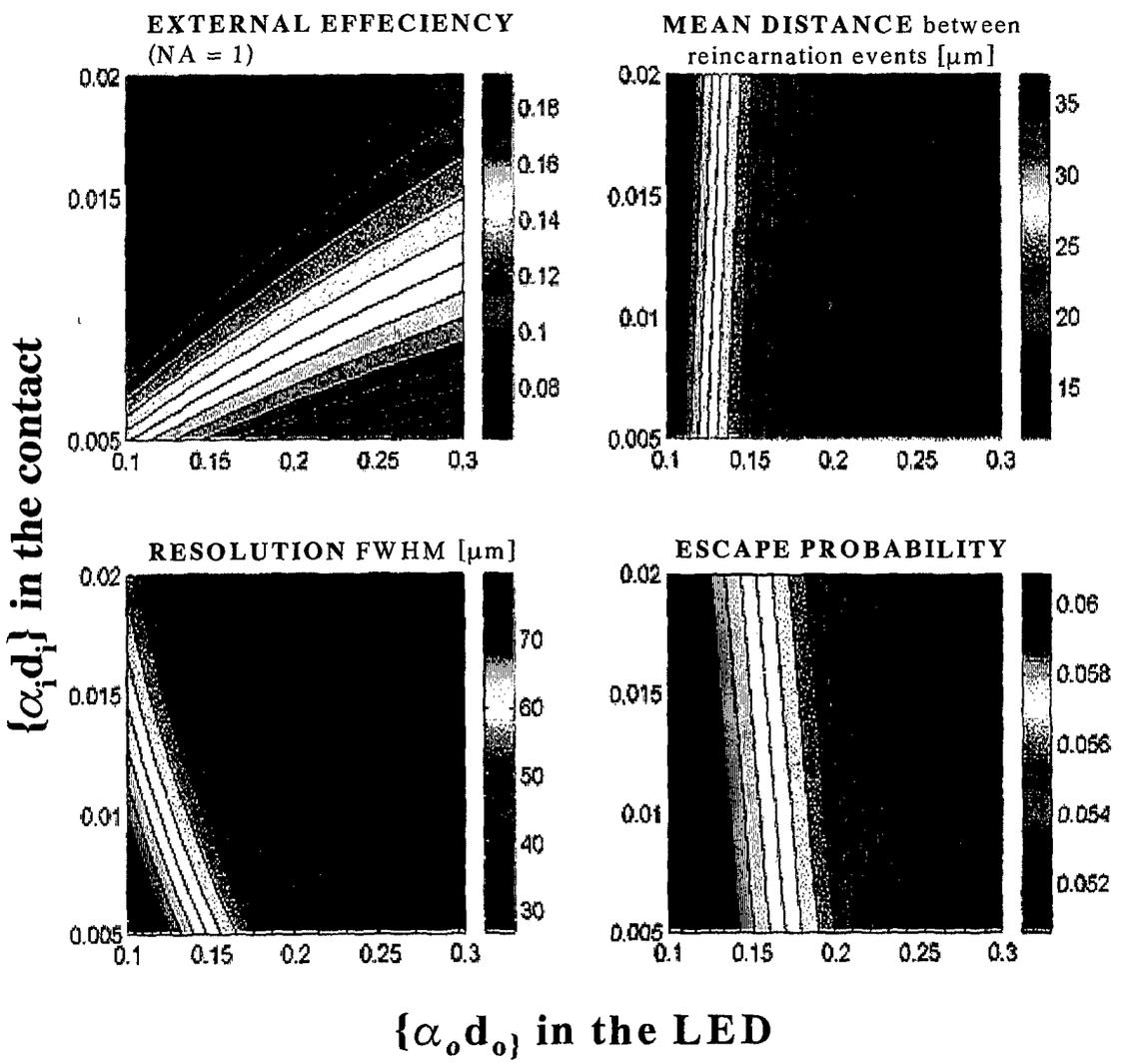

Fig. 9 Imperfect coatings: $\eta_{int} = 0.999$, T' = 0.7 (0° to θ_c), A' = 0 (0° to 90°), R = 0.7 (0° to 17°), and A = 0 (0° to 90°).

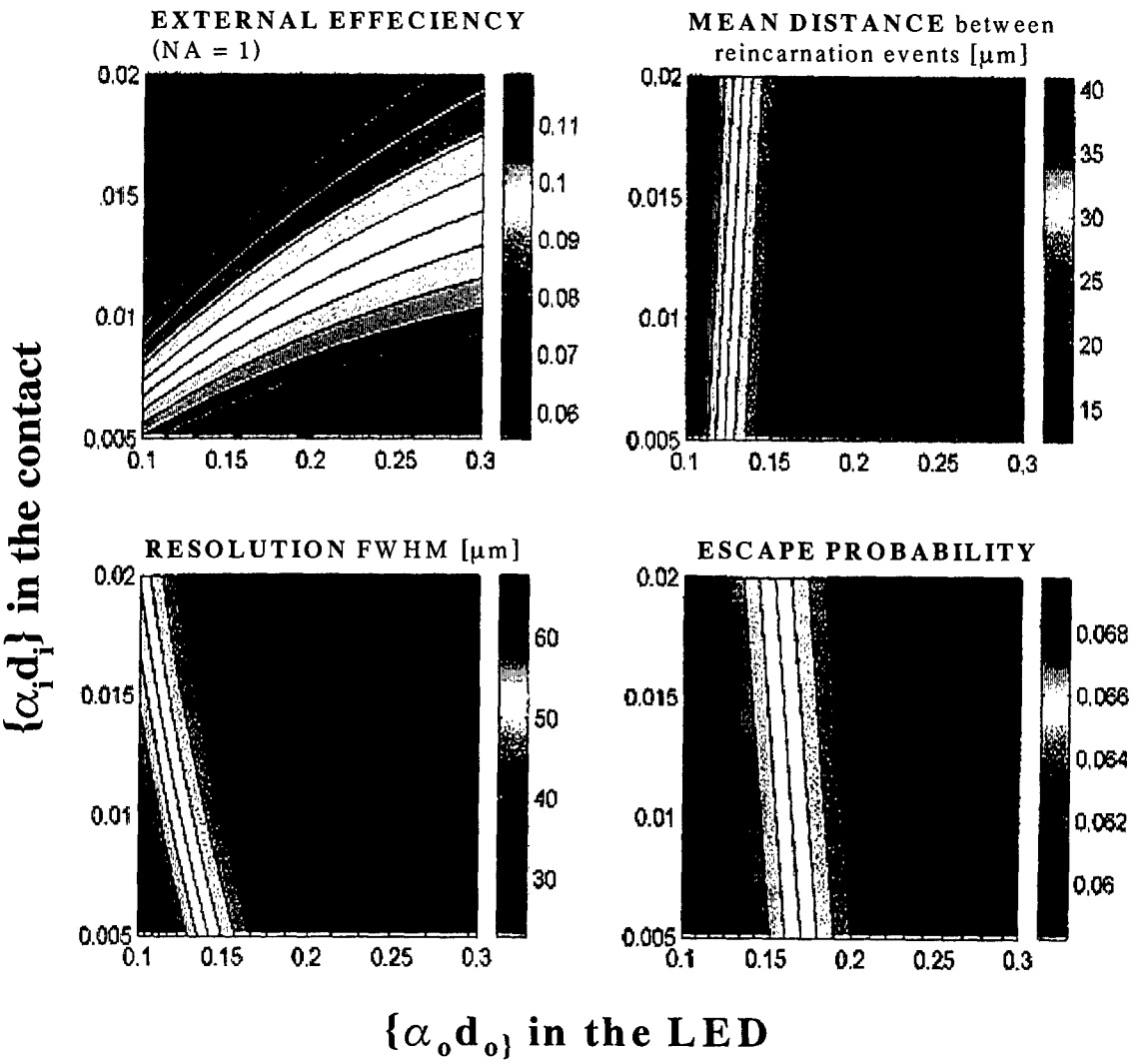

Fig. 10 Pessimistic case: $\eta_{int} = 0.95$, T' = 0.8 (0° to θ_c), A' = 0 (0° to 90°), R = 0.8 (0° to 17°), and A = 0 (0° to 90°).

7. Conclusions

We have studied the major device parameters influencing the NIR light lateral spread and the LED external efficiency of a QWIP-LED imaging device based on Schnitzer's LED model. The originality of this work was to try to estimate the crosstalk between M/FIR and NIR images. We found that the crosstalk is difficult to avoid and that the solution involves increasing the LED active region. However, the carrier diffusion length limits the maximum LED thickness to ~6000 Å. With a 1% absorption loss due the contacts, we expect a crosstalk to be around 30 μm and an external efficiency to be 10-15%. To further improve the external efficiency of these devices, we will most likely have to seriously consider bonding the QWIP-LED directly onto a CCD chip. Since the index of refraction of the CCD is very close to that of the LED, the escape cone will be significantly wider (~140°), allowing as much as 75-80% of the NIR light to escape at each emission event. This will not only drastically improve the external efficiency (up to 70-80%) but also will considerably reduce the crosstalk. The direct bonding option is presently being investigated by our research group as well as by CAL corporation as a part of a separate contract work.

Acknowledgements

The authors would like to thank Dr. H.C. Liu and Dr. M. Buchanan for their helpful comments and discussions. This work is supported by Defence Research Establishments, Valcartier and Ottawa, of Department of National Defence and Institute for Microstructural Science of National Research Council of Canada.

References

[1] W.R. Dyer and M.Z. Tidrow, "Infrared Sensor Technology to Ballistic Missile Defense," presented at 6th International Symposium on Long Wavelength Infrared Detectors and Arrays: Physics and Applications, Nov. 5-6, 1998, Boston, MA.

[2] H.C. Liu, J. Li, Z.R. Wasilewski, and M. Buchanan, Electron. Lett. *31*, 832 (1995).

[3] M. Ershov, H.C. Liu, and L.M. Schmitt, J. Appl. Phys. *82*, 1446 (1997).

[4] M. Ershov, Appl. Phys. Lett. *72*, 2865 (1998).

[5] R.J. Nelson and R.G. Sobers, J. Appl. Phys. *49*, 6103 (1978).

[6] I Schnitzer, E. Yablonovitch, C. Caneau, and T.J. Gmitter, Appl. Phys. Lett. *62*, 131 (1993).

[7] S. Chiu, C. Py, H.C. Liu, M. Buchanan, and E. Dupont, "A simple substrate removal process for a QWIP-LED device grown on GaAs," (to be published).

UNCLASSIFIED

SECURITY CLASSIFICATION OF FORM
(highest classification of Title, Abstract, Keywords)

DOCUMENT CONTROL DATA

(Security classification of title, body of abstract and indexing annotation must be entered when the overall document is classified)

1. **ORIGINATOR** (the name and address of the organization preparing the document. Organizations for whom the document was prepared, e.g. Establishment sponsoring a contractor's report, or tasking agency, are entered in section 8.)

Defence Research Establishment Ottawa
Ottawa,Ontario K1A 0Z4

2. **SECURITY CLASSIFICATION** (overall security classification of the document including special warning terms if applicable)

UNCLASSIFIED

3. **TITLE** (the complete document title as indicated on the title page. Its classification should be indicated by the appropriate abbreviation (S,C or U) in parentheses after the title.)

Image smearing in a quantum well infrared photodetector monolithically integrated with a light emitting diode (U)

4. **AUTHORS** (Last name, first name, middle initial)

Chiu, Shen (DREO/DND)
Dupont, Emmanuel (IMS/NRC)

5. **DATE OF PUBLICATION** (month and year of publication of document)

December 1998

6a. **NO. OF PAGES** (total containing information. Include Annexes, Appendices, etc.)

19

6b. **NO. OF REFS** (total cited in document)

7

7. **DESCRIPTIVE NOTES** (the category of the document, e.g. technical report, technical note or memorandum. If appropriate, enter the type of report, e.g. interim, progress, summary, annual or final. Give the inclusive dates when a specific reporting period is covered.

DREO Report

8. **SPONSORING ACTIVITY** (the name of the department project office or laboratory sponsoring the research and development. Include the address.

Space Systems and Technology Section
Defence Research Establishment Ottawa

9a. **PROJECT OR GRANT NO.** (if appropriate, the applicable research and development project or grant number under which the document was written. Please specify whether project or grant)

5ef12

9b. **CONTRACT NO.** (if appropriate, the applicable number under which the document was written)

10a. **ORIGINATOR'S DOCUMENT NUMBER** (the official document number by which the document is identified by the originating activity. This number must be unique to this document.)

DREO REPORT 1339

10b. **OTHER DOCUMENT NOS.** (Any other numbers which may be assigned this document either by the originator or by the sponsor)

11. **DOCUMENT AVAILABILITY** (any limitations on further dissemination of the document, other than those imposed by security classification)

(×) Unlimited distribution
( ) Distribution limited to defence departments and defence contractors; further distribution only as approved
( ) Distribution limited to defence departments and Canadian defence contractors; further distribution only as approved
( ) Distribution limited to government departments and agencies; further distribution only as approved
( ) Distribution limited to defence departments; further distribution only as approved
( ) Other (please specify):

12. **DOCUMENT ANNOUNCEMENT** (any limitation to the bibliographic announcement of this document. This will normally correspond to the Document Availability (11). however, where further distribution (beyond the audience specified in 11) is possible, a wider announcement audience may be selected.)

Unlimited announcement

UNCLASSIFIED

SECURITY CLASSIFICATION OF FORM

13. **ABSTRACT** (a brief and factual summary of the document. It may also appear elsewhere in the body of the document itself. It is highly desirable that the abstract of classified documents be unclassified. Each paragraph of the abstract shall begin with an indication of the security classification of the information in the paragraph (unless the document itself is unclassified) represented as (S), (C), or (U). It is not necessary to include here abstracts in both official languages unless the text is bilingual).

The recent advances in infrared sensing technology has made it possible to use infrared sensors to support environmental observations, surveillance, threat detection, tracking, and target identification. For ballistic missile defence (BMD) related applications, the most important detector requirements are: high sensitivity, high uniformity, large format, and multicolor capabilities. Quantum well infrared photodetector (QWIP) is a relatively new candidate technology for BMD applications. It has become one of the most promising near-term infrared technologies to meet mid-course detection requirements because of its wavelength flexibility in mid-infrared, far-infrared, and very far-infrared regions, as well as multicolor capabilities. Canadian QWIP technology is based on monolithic integration of quantum well infrared photodetector with a light emitting diode (QWIP-LED), and was pioneered by Dr. H.C. Liu of Institute for Microstructural Sciences, National Research Council of Canada. The goal of the present program is to realize a 1×1 cm^2 two-color QWIP-LED imaging device by March 2001 and, eventually, to develop a very large format (up to 4×4 cm^2) prototype imaging camera.

The success of the QWIP-LED depends critically on the extent of spatial lateral spreading of both photocurrent generated in the QWIP and near infrared photons emitted by the LED as they escape from the QWIP-LED layers. According to a LED model proposed by Schnitzer ***et al.***, there appears to be a trade-off between a high LED external quantum efficiency and a small photon lateral spread, the former being a necessary condition for achieving high detector sensitivity. The model predicts that as much as 25 reincarnations of the originally emitted NIR photons (as they spread laterally within the QWIP-LED) are required for most of the LED emitted light to escape. This lateral spreading due to multiple reflections and reincarnations of the NIR photons could potentially degrade the image quality or resolution of the QWIP-LED device. By adapting Schnitzer's model to the QWIP-LED structure, we have identified device parameters that could potentially influence the NIR photon lateral spread and the LED external efficiency. To achieve a high LED external efficiency we have found that the thickness of the LED active layer had to be significantly increased. Also, any additional absorption by anti-reflective coatings could have detrimental effects on the LED external efficiency. In addition, we have developed a simple sequential model to estimate the crosstalk between the incoming far (or mid) infrared image and the up-converted near infrared image. We found that the thickness of the LED is an important parameter that needs to be optimized in order to maximize the external efficiency and to minimize the crosstalk. A 6000 Å thick LED active layer should give a resolution of ~30 μm and an external efficiency of 10 to 15%.

14. **KEYWORDS, DESCRIPTORS or IDENTIFIERS** (technically meaningful terms or short phrases that characterize a document and could be helpful in cataloguing the document. They should be selected so that no security classification is required. Identifiers, such as equipment model designation, trade name, military project code name, geographic location may also be included. If possible keywords should be selected from a published thesaurus. e.g. Thesaurus of Engineering and Scientific Terms (TEST) and that thesaurus-identified. If it is not possible to select indexing terms which are Unclassified, the classification of each should be indicated as with the title.)

Quantum Well Infrared Photodetector (QWIP)
Light Emitting Diode (LED)
External quantum efficiency
Internal quantum efficiency
Photon lateral spread, image smearing, image resolution